Characterization of a wavelength-tunable antenna-coupled infrared microbolometer

Michael A. Gritz, MEMBER SPIE
Raytheon
Space and Airborne Systems
Electronic Warfare Systems
6380 Hollister Ave
Goleta, California 93117
E-mail: Michael_A_Gritz@raytheon.com

Meredith Metzler
Cornell University
Cornell NanoScale Facility
Ithaca, New York 14853-5403

Mohamed Abdel-Rahman
Brian Monacelli, MEMBER SPIE
Guy Zummo
University of Central Florida
CREOL/School of Optics
Orlando, Florida 32816-2700

Donald Malocha
University of Central Florida
Department of Electrical and Computer Engineering
Orlando, Florida 32816-2362

Glenn D. Boreman, MEMBER SPIE
University of Central Florida
CREOL/School of Optics
Orlando, Florida 32816-2700

Abstract. Wavelength tuning is demonstrated in an antenna-coupled infrared microbolometer. With a 300-mV control voltage, we observed a tuning range of 0.5 μm near 10 μm. A metal-oxide-semiconductor capacitor underneath the antenna arms causes the shift of resonance wavelength with applied voltage. We develop a device model that agrees well with measured results. [DOI: 10.1117/1.1869892]

Subject terms: microbolometer; antenna-coupled detectors; wavelength-tunable detectors.

Paper 040235 received May 4, 2004; accepted for publication Sep. 7, 2004; published online Mar. 23, 2005.

1 Introduction

Conventional bolometers have long been used as thermal detectors for infrared (IR) radiation, using the change of resistance with an increase in the temperature. In the case of antenna-coupled microbolometers,[1,2] incident radiation induces IR-frequency current waves in the arms of the antenna, which are dissipated in the subwavelength-size bolometer. One of the main advantages of antenna coupling of IR sensors is that their polarization[3] and wavelength responses can be electrically tuned by control of the current waves propagating on the antenna arms. In this paper we present the first demonstration of wavelength tuning in an antenna-coupled infrared microbolometer. The tuning mechanism is derived from a metal-oxide-semiconductor capacitor (MOS-C) underneath the arms of the antenna. Controlling the capacitance of this MOS-C by a small dc voltage modifies the electrical length of the antenna, thus tuning the free-space resonant wavelength.

2 Device Model

A cross section of the device along with its equivalent circuit is shown in Fig. 1, with full length of the antenna $b = 1.7\,\mu$m, cross-arm width $a = 0.385\,\mu$m, and distance from contact to feed point $d = 0.95\,\mu$m. The thickness h of the sputtered SiO_2 insulator layer is 25 nm, and the substrate is 8000-Ω-cm p-type Si with $N_A = 4\times10^{11}\,\mathrm{cm}^{-3}$.

A transmission-line model was developed for the combined antenna and MOS-C. The MOS-C acts as a varactor (C_{MOS}), in series with the antenna capacitance C_{a}. Their equivalent capacitance C_{Eq} is in parallel with the antenna inductance L_{a} and the fringe-field capacitance C_{f}. The resonance frequency f_r for the antenna is given by

$$f_r = \frac{1}{2\pi[L_{\mathrm{a}}(C_{\mathrm{Eq}} + C_{\mathrm{f}})]^{1/2}}, \tag{1}$$

where C_{Eq} is the series equivalent capacitance for the MOS-C and C_{t}, given by

$$C_{\mathrm{Eq}} = \frac{C_{\mathrm{a}} C_{\mathrm{MOS}}}{C_{\mathrm{a}} + C_{\mathrm{MOS}}}. \tag{2}$$

A computer model was developed to model the capacitance-voltage characteristics for a p-type MOS-C using an exact charge distribution model inside the MOS-C.[4] For the model a set of parameters must be introduced. The first parameter is the potential as a function of the depth x into the semiconductor, which is given by

$$U(x) = \frac{E_i(\mathrm{bulk}) - E_i(x)}{kT}, \tag{3}$$

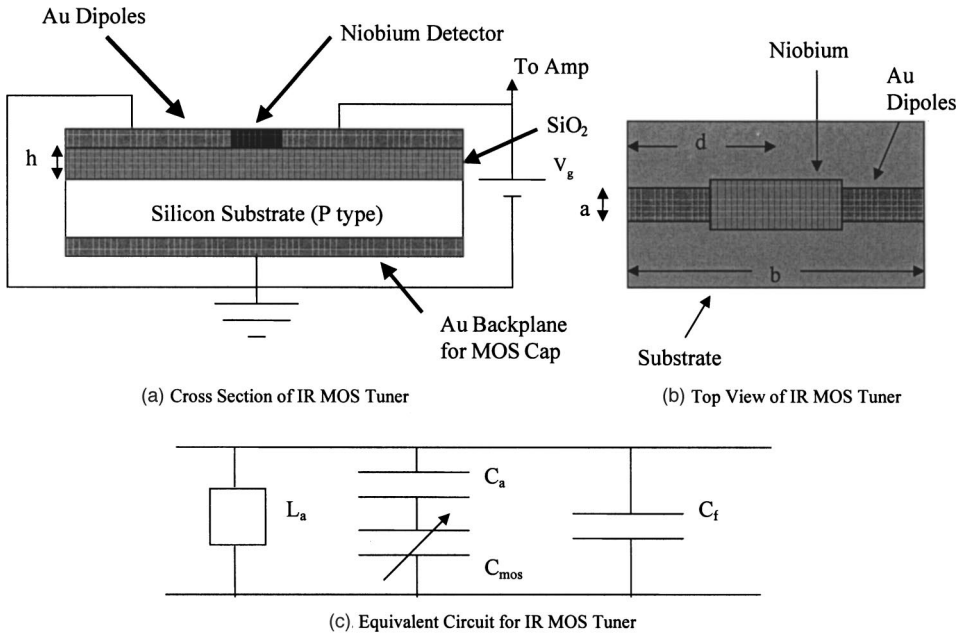

Fig. 1 IR MOS tuner: (a) cross section; (b) top view; (c) equivalent circuit.

where k is Boltzmann's constant and T is the temperature. The surface potential in the semiconductor is then

$$U_S=\frac{E_i(\text{bulk})-E_i(\text{surface})}{kT}. \tag{4}$$

The second parameter is the doping parameter, which is given by

$$U_F=\frac{E_i(\text{bulk})-E_F}{kT}. \tag{5}$$

In addition to the potentials, a quantitative expression for the band bending inside the semiconductor is formulated using the intrinsic Debye length. The Debye length was originally introduced in the study of plasmas.[4] Whenever a plasma is perturbed by placing a charge in it, the mobile species always rearrange so as to shield the plasma proper from the charge. The Debye length is the shielding distance. In the bulk, the semiconductor can be viewed as a plasma with an equal number of ionized impurity states and mobile electrons or holes. The placement of a charge near the semiconductor causes the mobile species inside the material to rearrange so as to shield the bulk semiconductor from the perturbing charge. The shielding distance is given by the bulk Debye length

$$L_B=\left[\frac{\epsilon_{\text{Si}}\epsilon_0 kT}{q^2(n_{\text{bulk}}+p_{\text{bulk}})}\right]^{1/2}, \tag{6}$$

where ϵ_{Si} and ϵ_0 are the dielectric constants in Si and free space, respectively, and q is the charge of an electron. The intrinsic Debye length L_D is found by setting $n_{\text{bulk}}=p_{\text{bulk}}=n_i$, where n_i is the intrinsic semiconductor concentration:

$$L_D=\left[\frac{\epsilon_{\text{Si}}\epsilon_0 kT}{2q^2 n_i}\right]^{1/2}. \tag{7}$$

The expressions for the charge density, electric field, and potential as a function of position inside the semiconductor are obtained by solving Poisson's equation:

$$\frac{\mathrm{d}\xi}{\mathrm{d}x}=\frac{\rho}{\epsilon_{\text{Si}}\epsilon_0}=\frac{q}{\epsilon_{\text{Si}}\epsilon_0}(p-n+N_D-N_A), \tag{8}$$

where ρ is the conductivity; p and n are the equilibrium doping concentrations in the semiconductor, which are given by

$$p=n_i\exp\{[E_i(x)-E_F]/kT\}=n_i\exp[U_F-U(x)], \tag{9}$$

$$n=n_i\exp\{[E_F-E_i(x)]/kT\}=n_i\exp[U(x)-U_F]; \tag{10}$$

and N_D and N_A are the nonequilibrium doping concentrations. Since the MOS-C is assumed to be a one-dimensional structure, Poisson's equation simplifies to

$$\xi=-\frac{kT}{q}\frac{\mathrm{d}U}{\mathrm{d}x}. \tag{11}$$

Since both ρ and U are zero in the semiconductor bulk,

$$N_D-N_A=n_i(e^{-U_F}-e^{U_F}). \tag{12}$$

Substituting Eqs. (9)–(12) into Eq. (8) results in

$$\rho=qn_i[\exp(U_F-U)-\exp(U-U_F)+e^{-U_F}-e^{U_F}] \tag{13}$$

and

$$\frac{d^2U}{dx}=\frac{q^2n_i}{\epsilon_{Si}\epsilon_0 kT}[\exp(U-U_F)-\exp(U_F-U)+e^{U_F}-e^{-U_F}]. \tag{14}$$

By substituting Eq. (7) into Eq. (14) one obtains

$$\frac{d^2U}{dx}=\frac{1}{2L_D^2}[\exp(U-U_F)-\exp(U_F-U)+e^{U_F}-e^{-U_F}]. \tag{15}$$

Poisson's equation, which is given in Eq. (8), is solved subject to the boundary conditions given below:

$$\xi=0, \text{ or } \frac{dU}{dx}=0, \quad \text{at } x=\infty \tag{16}$$

and

$$U=U_S \quad \text{at } x=0. \tag{17}$$

When both sides of Eq. (8) are multiplied by dU/dx and integrated from $x=\infty$ to an arbitrary point x, then using the boundary conditions one obtains

$$\xi^2=\left(\frac{kT/q}{L_D}\right)^2[e^{U_F}(e^{-U}+U-1)+e^{-U_F}(e^{U}-U-1)]. \tag{18}$$

Equation (18) is of the form $y^2=a^2$, which has two roots, $y=a$ and $y=-a$. The energy-band diagram indicates that we must have $\xi>0$ when $U>0$ and $\xi<0$ when $U<0$. Since the right-hand side of the equation is always positive ($a\geqslant 0$), the proper polarity for the electric field is obtained by choosing the positive root when $U>0$ and the negative root when $U<0$. Therefore we can write

$$\xi=\hat{U}_S\frac{kT}{q}\frac{F(U,U_F)}{L_D}, \tag{19}$$

where

$$F(U_S,U_F)=[e^{U_F}(e^{-U_S}+U_S-1)+e^{-U_F}(e^{U_S}-U_S-1)]^{1/2} \tag{20}$$

and

$$\hat{U}_S=\begin{cases}+1 & \text{if } U_S>0,\\ -1 & \text{if } U_S<0.\end{cases} \tag{21}$$

Now the capacitance can be found using

$$C=\frac{C_o}{1+\epsilon_{SiO_2}W_{eff}/\epsilon_{Si}h}, \tag{22}$$

where C_o is the oxide capacitance and W_{eff} is the effective width of the depletion region and is given by

$$W_{eff}=\begin{cases}U_SL_D\left[\dfrac{2F(U_S,U_F)}{e^{U_F}(1-e^{-U_S})+e^{-U_F}(e^{U_S}-1)}\right] & \text{(accumulation region)},\\ \dfrac{\sqrt{2}L_D}{(e^{U_F}+e^{-U_F})^{1/2}} & \text{(flat band)},\\ U_SL_D\left[\dfrac{2F(U_S,U_F)}{e^{U_F}(1-e^{-U_S})+e^{-U_F}(e^{U_S}-1)}\right] & \text{(depletion region, inversion)}.\end{cases} \tag{23}$$

Since we are using an exact charge distribution model, the capacitance cannot be expressed as a function of the applied voltage. However, both variables are related to U_S; therefore, the capacitance expected for a given applied voltage, including the metal-semiconductor work-function difference, can be found using

$$V_G=\frac{kT}{q}\left[U_S+\hat{U}_S\frac{\epsilon_{Si}h}{\epsilon_{SiO_2}L_D}F(U_S,U_F)+\phi_{Au}-\ln\left(\frac{N_A}{n_i}\right)-\frac{E_g}{2}\right], \tag{24}$$

where $\phi_{Au}=0.7\,\text{eV}$ is the work function for gold, $n_i=1.5\times10^{10}\,\text{cm}^{-3}$ is the intrinsic concentration of Si, and $E_g=1.1\,\text{eV}$ is the bandgap energy of Si.

Now we model the equivalent capacitance C_{Eq} as a function of voltage, using

$$C_{Eq}=\frac{C_a}{1+\epsilon_{SiO_2}W_{eff}/\epsilon_{Si}h}. \tag{25}$$

This equation can be evaluated once we know C_a of the microstrip dipole antenna, which can be found using[5]

$$C_a=\frac{\epsilon_0\epsilon_r ab}{2h}\cos^{-2}\left(\frac{\pi d}{b}\right), \tag{26}$$

where the average relative permittivity ϵ_r of the substrate is calculated as

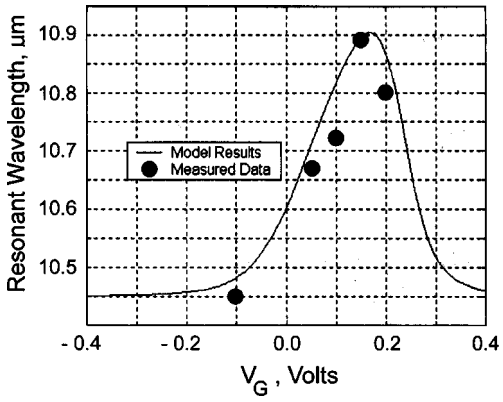

Fig. 2 Comparison of model and measured data for the wavelength-tuned antenna.

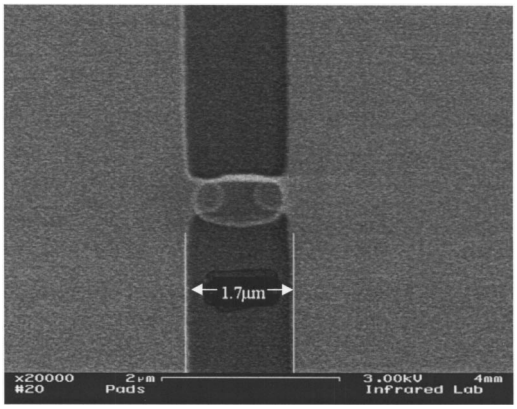

Fig. 3 Scanning electron micrograph of a 1.7-μm dipole-antenna-coupled microbolometer IR MOS tuner.

$$\epsilon_r = \frac{\epsilon_{SiO_2}\epsilon_{Si}}{\epsilon_{SiO_2} + \epsilon_{Si}}. \tag{27}$$

The inductance L_a of the antenna can be calculated from Eq. (1) as

$$L_a = \frac{1}{\omega^2 C_{eq}}. \tag{28}$$

For calculation of the fringe-field capacitance C_f, we consider that the microstrip has electrical dimensions greater than its physical dimensions. For the antenna shown in Fig. 1, the fringing affects the cross-arm width a of the dipole. The difference is found as[6]

$$\Delta a = 0.412h \frac{(\epsilon_r + 0.3)(a/h + 0.264)}{(\epsilon_r - 0.258)(a/h + 0.8)}. \tag{29}$$

Now C_f can be found, using[5]

$$C_f = \frac{0.01668\epsilon_r}{\omega}\left(\frac{\Delta a}{h}\right)\left(\frac{a}{\lambda_r}\right), \tag{30}$$

where $\lambda_r = 10.45\ \mu$m is the initial measured resonant wavelength.

Using Eq. (1), with results from Eqs. (25), (26), (28), and (30), allows us to find the free-space resonant wavelength ($\lambda = c/f$) of the IR MOS tuner as function of applied voltage V_G. The results of this model are shown in Fig. 2, along with measured values. When the device was biased beyond 150 mV, its resonance began to shift towards shorter wavelengths.

3 Fabrication of the Tuner

The IR MOS tuners were fabricated at the Cornell Nano-Scale Facility using a Cambridge/Leica EBMF 10.5 e-beam lithography system. The dipole-antenna-coupled microbolometer was fabricated on top of a 3-in. Si wafer with a resistivity of 8000 Ω cm ($N_A = 4\times10^{11}\ \mathrm{cm}^{-3}$). Both local and global alignment marks were then written using a bilayer of poly(methylmethacrylate and methacrylic acid) (PMMA-MAA) and poly(methylmethacrylate) (PMMA) in a liftoff process. The global marks were used to correct for any rotation errors while loading the substrates into the chuck, while the local marks were used to correct for any stage drift when moving from field to field. Gold was used for the dipole antenna arms, with niobium as the bolometer. We fabricated the MOS-C with 25 nm of sputtered SiO_2 on top of a *p*-type Si substrate, and used a dipole antenna with a full antenna length of 1.7 μm. The width of the antenna arms as fabricated was 385 nm. A scanning electron micrograph of one of the devices fabricated is shown in Fig. 3.

4 Tuning Measurements

We used a tunable CO_2 laser with emission from 9.28 to 10.78 μm in discrete lines. The laser was focused by an f/1 optical train. The laser polarization was linear and was rotated by means of a half-wave plate. The bolometer under test was placed at the focus of the beam. The position of the device was adjusted for the best response by using motorized stages with submicron accuracy. The beam was modulated with a chopper at a frequency of 2.5 kHz. The modulated signal was read with a lock-in amplifier after a 10× preamplification. For the device under test, the maximum signal V_{max} was obtained for the polarization parallel to the antenna axis, and the minimum signal V_{min} was obtained for the cross polarization. The polarization-dependent signal is defined as $\Delta V = V_{max} - V_{min}$. The polarization-dependent signal and the power on the detector were measured for each wavelength. The power fluctuation from the laser output for each wavelength was removed from the measured signal by normalization of the polarization signal (volts) to the measured power (watts) on the detector.

The bolometer under test was biased with both positive (depletion mode) and negative voltages (accumulation mode) and placed at the focus of the beam. The device was first measured with a bias of −100 mV. Then a positive bias was applied, which was adjusted in 50-mV increments up to 200 mV. The discrete-line results of each measurement were then fitted with a Gaussian profile using a least-squares fit in order to find the precise resonance of the dipole antenna at each bias voltage. These data for resonance wavelength as a function of bias voltage are seen in Fig. 2.

5 Conclusions

An antenna-coupled IR bolometer was demonstrated to have tunable wavelength reponse near 10 μm, with around 0.5 μm of tuning. The tuning mechanism is an MOS capacitor developed underneath the antenna structure in a Si substrate. A model was developed for the tuning behavior that agrees well with measured values. Trends in this model indicate that the tuning range is increased for thinner oxide layers and for lower doping concentrations. Our device was thus fabricated with an oxide layer of 25 nm and a substrate resistivity of 8000 Ω cm.

Acknowledgments

This work was performed in part at the Cornell Nanofabrication facility (a member of the National Nanofabrication Users Network), which is supported by the National Science Foundation under grant No. ECS-9731293, Cornell University, and industrial affiliates. This material is based on research supported by NASA grant NAG5-10308.

References

1. E. Grossman, J. Sauvageau, and D. McDonald, ''Lithographic spiral antennas at short wavelengths,'' *Appl. Phys. Lett.* **59**, 3225–3227 (1991).
2. I. Codreanu, C. Fumeaux, D. Spencer, and G. Boreman, ''Microstrip antenna-coupled infrared detector,'' *Electron. Lett.* **35**, 2166–2167 (1999).
3. G. Boreman, C. Fumeaux, W. Herrmann, F. Kneubühl, and H. Rothuizen, ''Tunable polarization response of a planar asymmetric-spiral infrared antenna,'' *Opt. Lett.* **23**, 1912–1914 (1998).
4. R. F. Pierret, *Semiconductor Device Fundamentals*, Chapter 16, Addison-Wesley, New York (1996).
5. S. K. Sharma and B. R. Vishvakarma, ''MOS capacitor loaded frequency agile microstrip antenna,'' *Int. J. Electron.* **86**, 979–990 (1999).
6. C. Balanis, *Antenna Theory Analysis and Design*, Chapter 4, Wiley, New York (1997).

Mohamed R. AbdelRahman received his BSc degree in physics from the American University in Cairo, Egypt in 1999 and his MSc and PhD degrees in electrical engineering from the University of Central Florida, Orlando, Florida, in 2002 and 2004 respectively. He served as a graduate research assistant in the Infrared Systems Laboratory at the College of Optics and Photonics (CREOL) from 2000 until 2004. His research interest is in the area of antenna-coupled detectors for millimeter-wave and infrared focal plane arrays. He is a member of SPIE.

Glenn D. Boreman is Trustee Chair Professor of Optics, Electrical Engineering, and Physics at the College of Optics and Photonics (CREOL) at the University of Central Florida. He received a BS from the Institute of Optics, University of Rochester, and a PhD from the Optical Sciences Center, University of Arizona. He has been a visiting scholar at Imperial College in London, the Swiss Federal Institute of Technology (ETH) in Zürich, and the Defense Research Agency (FOI) in Linköping, Sweden. Dr. Boreman currently serves as the Editor-in-Chief of OSA's journal *Applied Optics*, and is a past member of the SPIE Board of Directors. He is coauthor of the graduate textbook *Infrared Detectors and Systems*, author of *Modulation Transfer Function in Optical & Electro-Optical Systems*, and *Basic Electro-Optics for Electrical Engineers*. He has published more than 100 articles in the areas of infrared detector and focal-plane analysis, optics of random media, infrared scene projection, and transfer-function techniques. Dr. Boreman is a Fellow of SPIE and OSA. He and two of his students received the 1995 Kingslake Medal from SPIE.

Biographies and photographs of other authors not available.